Quantitative Evaluation of the Contribution of Each Aldo-Keto Reductase and Short-Chain Dehydrogenase/Reductase Isoform to Reduction Reactions of Compounds Containing a Ketone Group in the Human Liver

Hiroyuki Ichida, Tatsuki Fukami, Keito Amai, Kohei Suzuki, Kenji Mishiro, Shiori Takano, Wataru Obuchi, Zhengyu Zhang, Akiko Watanabe, Masataka Nakano, Kengo Watanabe, and Miki Nakajima

Drug Metabolism and Toxicology, Faculty of Pharmaceutical Sciences (H.I., T.F., K.A., K.S., S.T., Ma.N., Mi.N.), WPI Nano Life Science Institute (WPI-NanoLSI) (T.F., Ma.N., Mi.N.), and Institute for Frontier Science Initiative (K.M.), Kanazawa University, Kanazawa, Japan; and Drug Metabolism and Pharmacokinetics Research Laboratories, Daiichi Sankyo Co., Ltd, Tokyo, Japan (W.O., Z.Z., A.W., K.W.)

ABSTRACT

Enzymes of the aldo-keto reductase (AKR) and short-chain dehydrogenase/reductase superfamilies are involved in the reduction of compounds containing a ketone group. In most cases, multiple isoforms appear to be involved in the reduction of a compound, and the enzyme(s) that are responsible for the reaction in the human liver have not been elucidated. The purpose of this study was to quantitatively evaluate the contribution of each isoform to reduction reactions in the human liver. Recombinant cytosolic isoforms were constructed, i.e., AKR1C1, AKR1C2, AKR1C3, AKR1C4, and carbonyl reductase 1 (CBR1), and a microsomal isoform, 11β-hydroxysteroid dehydrogenase type 1 (HSD11B1), and their contributions to the reduction of 10 compounds were examined by extrapolating the relative expression of each reductase protein in human liver preparations to recombinant systems quantified by liquid chromatography–mass spectrometry. The reductase activities for acetohexamide, doxorubicin, haloperidol, loxoprofen, naloxone, oxcarbazepine, and pentoxifylline were predominantly catalyzed by cytosolic isoforms, and the sum of the contributions of individual cytosolic reductases was almost 100%. Interestingly, AKR1C3 showed the highest contribution to acetohexamide and loxoprofen reduction, although previous studies have revealed that CBR1 mainly metabolizes them. The reductase activities of bupropion, ketoprofen, and tolperisone were catalyzed by microsomal isoform(s), and the contributions of HSD11B1 were calculated to be 41%, 32%, and 104%, respectively. To our knowledge, this is the first study to quantitatively evaluate the contribution of each reductase to the reduction of drugs in the human liver.

SIGNIFICANCE STATEMENT

To our knowledge, this is the first study to determine the contribution of aldo-keto reductase (AKR)-1C1, AKR1C2, AKR1C3, AKR1C4, carbonyl reductase 1, and 11β-hydroxysteroid dehydrogenase type 1 to drug reductions in the human liver by utilizing the relative expression factor approach. This study found that AKR1C3 contributes to the reduction of compounds at higher-than-expected rates.

Introduction

Most administered drugs are metabolized mainly in the liver and intestines by oxidation, reduction, hydrolysis, or conjugation. Reduction reactions account for 2.2% of the metabolic reactions of clinical drugs (Fukami et al., 2022). In particular, compounds containing ketone, nitro, and sulfoxide groups undergo reduction reactions. Although cytochrome P450s, which are major drug-metabolizing enzymes, catalyze not only oxidation reactions but also reduction reactions, the drugs reduced by cytochrome P450 are limited (Zangar et al., 2000). Most reduction reactions of the ketone groups in compounds are catalyzed by enzymes belonging to the aldo-keto reductase (AKR) and short-chain dehydrogenase/reductase (SDR) superfamilies. In humans, there are 15 AKR isoforms—AKR1A1, AKR1B1, AKR1B10, AKR1B15, AKR1C1, AKR1C2, AKR1C3, AKR1C4, AKR1D1, AKR1E2, AKR6A3, AKR6A5, AKR6A9, AKR7A2, and AKR7A3 (www.med.upenn.edu/akr)—and 75 SDR isoforms (Persson and Kallberg, 2013), including carbonyl reductase (CBR)-1 (SDR21C1), CBR3 (SDR21C2), CBR4 (SDR45C1), 11β-hydroxysteroid dehydrogenase type 1 (HSD11B1, SDR26C1), dehydrogenase/reductase member 4 (SDR25C2), and dicarbonyl/L-xylulose reductase (SDR20C1). Among them, 12 AKR isoforms—with

ABBREVIATIONS: AKR, aldo-keto reductase; CBR, carbonyl reductase; CL_{int}, intrinsic clearance; DCM, dichloromethane; G6P, glucose-6-phosphate; HLC, human liver cytosol; HLM, human liver microsomes; HPLC, high-performance liquid chromatography; HSD11B1, 11β-hydroxysteroid dehydrogenase type 1; K_m, Michaelis constant; LC-MS/MS, liquid chromatography-tandem mass spectrometry; MRM, multiple reaction monitoring; REF, relative expression factor; SDR, short-chain dehydrogenase/reductase; $V_{predicted}$ S-V, substrate concentration vs catalytic velocity, predicted activity of human liver reductase.

the exception of AKR6A3, AKR6A5, and AKR6A9—and six SDR isoforms, CBR1, CBR3, CBR4, HSD11B1, dehydrogenase/reductase member 4, and dicarbonyl/$_L$-xylulose reductase, have been considered to participate in the reduction of xenobiotics (Matsunaga et al., 2006).

In most cases, multiple isoforms appear to be involved in compound reduction. For example, doxorubicin has been reported to be reduced to doxorubicinol by AKR1A1, AKR1B1, AKR1B10, AKR1C3, AKR1C4, and CBR1 (Kassner et al., 2008), but the enzyme with the highest contribution to doxorubicin reduction in the human body has not been elucidated. Although Kishimoto et al. (1994) showed—in an inhibition study using several inhibitors—that acetohexamide reduction in erythrocytes is mainly catalyzed by CBR1, Ohara et al. (1995) reported that this reaction was not catalyzed by purified human CBR1. Dalmadi et al. (2003) revealed tolperisone reduction by human liver microsomes (HLM), but the responsible enzyme(s) were not identified. Thus, there was hardly any progression in the identification of the enzyme(s) responsible for each reduction reaction. Estimation of the contribution of each isoform to the reduction of compounds of interest is helpful for predicting interindividual differences in drug efficacy or drug-drug interactions.

Recently, we evaluated the mRNA levels of 12 AKR and 6 SDR isoforms in the human liver and demonstrated that AKR1C1, AKR1C2, AKR1C3, CBR1, and HSD11B1 were expressed at over 10% of the total reductase expression, and the sum of these five isoforms reached 64.5% (Amai et al., 2020). AKR1C4 is moderately expressed (5.6% of the total reductase expression levels) (Amai et al., 2020). Early studies demonstrated that AKR1C1, AKR1C2, AKR1C3, AKR1C4, CBR1, and HSD11B1 can catalyze drug reduction reactions (Ohara et al., 1995; Matsunaga et al., 2006; Meyer et al., 2013). Therefore, we sought to quantitatively evaluate the contributions of these isoforms to the reduction reactions of 10 representative compounds containing a ketone group in the human liver.

Materials and Methods

Chemicals and Reagents. Acetohexamide, dihydro ketoprofen, doxorubicin hydrochloride, ketoprofen, haloperidol, loxoprofen sodium hydrate, and tolperisone hydrochloride were purchased from FUJIFILM Wako Pure Chemical (Osaka, Japan). Bupropion and naloxone hydrochloride were purchased from Sigma-Aldrich (St. Louis, MO). Doxorubicinol, lisofylline, reduced haloperidol, *erythro*-dihydro bupropion, and *threo*-dihydro bupropion were purchased from Toronto Research Chemicals (Toronto, Canada). Oxcarbazepine, hydroxyhexamide, and 6β-naloxol were purchased from LKT Laboratories (St. Paul, MN), Medchem Express (Tokyo, Japan), and Cayman Chemical (Ann Arbor, MI), respectively. *trans*-Hydroxyloxoprofen and *cis*-hydroxyloxoprofen were obtained from Daiichi Sankyo (Tokyo, Japan). Glucose-6-phosphate (G6P), G6P dehydrogenase, and β-nicotinamide adenine dinucleotide phosphate (NADP$^+$) were obtained from Oriental Yeast (Tokyo, Japan). The rabbit anti-human HSD11B1 polyclonal antibody was purchased from Boster Biologic Technology (Pleasanton, CA). IRDye 680-labeled goat anti-rabbit IgG and Odyssey blocking buffer were purchased from LI-COR Biosciences (Cambridge, UK). Immobilon-P PVDF membranes were purchased from Millipore (Billerica, MA). Human liver cytosol [pooled human liver cytosol (HLC), $n = 150$ (male, $n = 75$; female, $n = 75$)] and human liver microsomes [pooled HLM, $n = 50$ (male, $n = 25$; female $n = 25$)] were purchased from Corning (Corning, NY). All other chemicals and solvents were of analytical grade or of the highest grade commercially available.

Synthesis of Dihydrotolperisone. To a stirred suspension of lithium aluminum hydride (80.8 mg, 2.13 mol) prepared in dry tetrahydrofuran (10 mL), tolperisone hydrochloride (300 mg, 1.06 mmol) was added at 0°C. After stirring at 0°C for 1 hour, complete consumption of tolperisone was confirmed by TLC. The reaction mixture was poured into ice-cold water. The mixture was extracted with ethyl acetate, and the extract was dried over Na_2SO_4. Na_2SO_4 was removed by filtration, and the filtrate was concentrated under reduced pressure to obtain a mixture of *threo*- and *erythro*-dihydrotolperisone as a colorless oil. The crude

material was analyzed by reversed-phase high-performance liquid chromatography (HPLC) with a Cosmosil 5C$_{18}$-mass spectrometry (MS)-II column (4.6 × 150 mm; Nacalai Tesque, Kyoto, Japan) at a flow rate of 1 mL/min with an isocratic mobile phase of 80% methanol in water with 0.05% triethylamine. Diastereomers 1 and 2 appeared at 6.4 and 6.9 minutes, respectively. The crude material was then purified by recycling a preparative HPLC system with a Cosmosil 5C$_{18}$-MS-II column (20 × 250 mm; Nacalai Tesque) at a flow rate of 14 mL/min with an isocratic mobile phase of 85% methanol in water with 0.05% triethylamine. As HPLC purification was not sufficient to separate the diastereomers, the obtained materials were converted to hydrochloride salts and purified by washing with an organic solvent. The purified products were analyzed by ^{1}H NMR spectroscopy with a JNM-ESC600 spectrometer (JEOL, Tokyo, Japan).

Fractions containing diastereomer 1 as the major compound were concentrated to afford colorless oil. The oil was dissolved in dichloromethane (DCM) (1.0 mL), and 4 M HCl in AcOEt (0.5 mL, 2.0 mmol) was added to the DCM solution. The mixture was concentrated to obtain a colorless solid. The solid was washed with DCM:hexane (1:4) to give the hydrochloride salt of dihydrotolperisone diastereomer 1 as a colorless solid (125 mg). The product was characterized by ^{1}H NMR [(600 MHz, CD$_3$OD) δ 7.25 (d, $J = 7.8$ Hz, 2H), 7.18 (d, $J = 7.8$ Hz, 2H), 4.77 (d, $J = 4.2$ Hz, 1H), 3.56 (br s, 2H), 3.34–3.25 (m, 3H), 3.18 (dd, $J = 13.2$, 4.8 Hz, 1H), 3.15–2.78 (m, 3H), 2.46–2.37 (m, 1H), 2.33 (s, 3H), 2.10–1.40 (m, 6H), 0.92 (d, $J = 6.6$ Hz, 3H)]. The product purity was 99% (confirmed by quantitative nuclear magnetic resonance using 1,3,5-trimethoxybenzene as the internal standard). Upon taking the purity into account, the yield of diastereomer 1 was 41%.

Fractions containing diastereomer 2 as the major compound were concentrated to obtain colorless oil. The oil was dissolved in DCM (1.0 mL), and 4 M HCl in AcOEt (0.5 mL, 2.0 mmol) was added to the DCM solution. The mixture was concentrated to obtain a colorless solid. The solid was washed with DCM/hexane (1/4) to obtain the hydrochloride salt of dihydrotolperisone diastereomer 2 as a colorless solid (101 mg). The product was characterized by ^{1}H NMR [(600 MHz, CD$_3$OD) δ 7.27 (d, $J = 7.8$ Hz, 2H), 7.19 (d, $J = 7.8$ Hz, 2H), 4.43 (d, $J = 9.6$ Hz, 1H), 3.86 (br d, $J = 12.0$ Hz, 1H), 3.55 (br d, $J = 12.0$ Hz, 1H), 3.18 (dd, $J = 13.2$, 6.0 Hz, 1H), 3.05–2.86 (m, 2H), 2.41–2.30 (m, 1H), 2.33 (s, 3H), 2.05–1.50 (m, 6H), 0.72 (d, $J = 6.6$ Hz, 3H)]. Product purity was 90% (confirmed by qNMR using 1,3,5-trimethoxybenzene as the internal standard). Upon taking the purity into account, the yield of diastereomer 2 was 30%.

Construction of Recombinant Human AKR1C1, AKR1C2, AKR1C3, AKR1C4, CBR1, and HSD11B1 To Be Expressed in Sf21 Cells. The expression systems for human AKR1C1, AKR1C2, AKR1C3, AKR1C4, CBR1, and HSD11B1 were constructed using a Bac-to-Bac Baculovirus Expression System (Invitrogen, Carlsbad, CA). The cDNAs of six enzymes were prepared by reverse-transcription polymerase chain reaction using total RNA purified from human liver samples obtained from the National Disease Research Interchange (Philadelphia, PA) through the Human and Animal Bridging Research Organization (Chiba, Japan). Reverse-transcription polymerase chain reaction products amplified with the primers listed in Table 1 were subcloned into the pFastBac1 vector. The pFastBac1 vectors were transformed into DH10Bac competent cells, followed by transposition of the inserts into bacmid DNA. The recombinant bacmid was transfected into *Spodoptera frugiperda* Sf21 cells. Other steps were performed in accordance with a method previously described (Fukami et al., 2010). Mock sample was also prepared by transfection with a nonrecombinant bacmid DNA. Protein concentration was determined using the method proposed by Bradford (1976) using γ-globulin as a standard.

Immunoblot Analysis of AKR1C1, AKR1C2, AKR1C3, AKR1C4, CBR1, and HSD11B1 Proteins. SDS-PAGE and immunoblot analysis were performed by referring to methods reported previously (Honda et al., 2021). HLC and HLM (2 μg) as well as recombinant enzymes (rAKR1C1, rAKR1C2, rAKR1C4, and rCBR1:2 μg, rAKR1C3:5 μg, rHSD11B1:2.5 μg) were separated on 7.5% SDS-PAGE and transferred to an Immobilon-P transfer membrane. The membranes were probed with monoclonal mouse anti-human AKR1C1 antibody (R&D Systems, Minneapolis, MN), monoclonal mouse anti-human AKR1C3 antibody (Sigma-Aldrich), polyclonal sheep anti-human AKR1C4 antibody (R&D Systems), polyclonal rabbit anti-CBR1 antibody (Bethyl Laboratories, Montgomery, AL), polyclonal rabbit anti-human HSD11B1 antibody (Boster Biologic Technology, Wuhan, China), and the corresponding fluorophore-conjugated secondary antibody. The bands were visualized by using an Odyssey infrared imaging

TABLE 1

Primer sequences used for the construction of expression plasmids *The nucleotide numbering refers to the transcription start site as 1.*

Isoform		Sequence'(5′ → 3′)	Product Size (bp)	Region	Ref. Seq
AKR1C1	S	GAAAGAAACATTTGCCAGCC	1144	149–1292	NM_001353
	AS	TGCTGTAGCTTGCTGAAATCA			
AKR1C2	S	CCACAGGTAAGAAACGGTTGA	1294	229–1522	NM_001354
	AS	AGCTGTAGCTTACTGAAGTCG			
AKR1C3	S	CAGACAAGTGACAGGGAATGGA	1019	53–1071	NM_003739
	AS	TCTGGTAGACATCAGGCAAAGC			
AKR1C4	S	AGTGGCAAGCAATGGATC	1015	23–1037	NM_001818
	AS	CTTCTGCTAGATGTCGTGC			
CBR1	S	TTCTCCACGCAGGTGTTC	1078	157–1234	NM_001757
	AS	GCATCAGAGGAAATCACAAAAG			
HSD11B1	S	GTCCTACAGGAGTCTTCAGGC	0928	120–1047	NM_005525
	AS	CCCTCAGGGAGTTCCTACTTG			

system (LI-COR Biosciences, Lincoln, NE). HLM and recombinant HSD11B1 were deglycosylated using Endo H in accordance with a previously reported method (Muta et al., 2014) and subjected to SDS-PAGE and immunoblot analysis.

Quantification of the Protein Levels of Reductases in Human Liver Fractions and Expression Systems. Absolute protein levels of AKR1C1, AKR1C2, AKR1C3, AKR1C4, CBR1, and HSD11B1 in the HLC, HLM, and recombinant systems were determined using liquid chromatgraphy-tandem mass spectrometry (LCMS/MS). The amino acid sequences and product ions used for the quantification of each reductase protein are listed in Table 2. The HLC, HLM, and recombinant samples were diluted with SDS and incubated at 100°C for 10 minutes. Fifty micrograms of the sample was carbamidomethylated with dithiothreitol, followed by treatment with iodoacetamide. Alkylated proteins were precipitated using a mixture of ice-cold methanol, chloroform, and water. The precipitates were dissolved in 8 M urea/Tris-EDTA solution, diluted with 0.1 M Tris-HCl (pH 8.0), and digested with a Trypsin/Lys-C mixture at an enzyme/substrate ratio of 1:100 at 37°C for 16 hours. The digested samples were mixed with stable isotope-labeled peptides and acidified with formic acid. The supernatants were evaluated using an liuquid chromatography system (Eksigent Ekspert NanoLC 400; SCIEX, MA) equipped with a ChromXP C18 column (3 μM, 500 μM I.D × 10 cm; SCIEX) connected to a mass spectrometer (TripleTOF 6600; SCIEX). Elution was performed using a mixture of solvent A, consisting of purified water and formic acid (1000:1, v/v), and solvent B, consisting of acetonitrile and formic acid (1000:1, v/v), as the mobile phase. MultiQuant software 3.0.3 (SCIEX) was used for data analysis. The levels of each protein in the pooled HLC, HLM, and expression systems were evaluated using two multiple reaction monitoring (MRM) modes. The relative expression factor (REF) for each reductase was calculated as follows:

$$REF = \frac{\text{Expression level in pooled HLC or HLM}}{\text{Expression level in expression system}} \quad (1)$$

The average REF values evaluated using two kinds of MRM modes were used to calculate the contribution.

Measurement of Reductase Activities for 10 Compounds Containing a Ketone Group. The reductase activities of 10 compounds (Fig. 1) were measured as follows: a typical incubation mixture (final volume of 0.2 mL) containing 100 mM potassium phosphate buffer (pH 7.4), enzyme sources (HLC, HLM, or recombinant reductases), and the substrate was prepared. Acetohexamide, bupropion, haloperidol, ketoprofen, and oxcarbazepine were

dissolved in DMSO, and doxorubicin hydrochloride, loxoprofen sodium hydrate, naloxone hydrochloride, pentoxifylline, and tolperisone hydrochloride were dissolved in distilled water. The final concentration of DMSO in the incubation mixture was adjusted to 1%. The assay conditions were determined such that the protein concentration and incubation time were linear (Table 3). The substrate concentrations were set near the Michaelis constant (K_m) values identified in this study (Table 3). After preincubation at 37°C for 2 minutes, reactions were initiated by the addition of an NADPH-generating system (5 mM G6P, 0.5 mM NADP$^+$, 5 mM MgCl$_2$, and 1 U/mL G6P dehydrogenase). After incubation at 37°C for the incubation time shown in Table 3, the reaction was terminated by the addition of 0.1 mL of ice-cold acetonitrile (the exception being naloxone, for which ice-cold methanol was used). The mixture was then centrifuged at 20,380*g* for 5 minutes.

For the measurement of reductase activities of nine compounds—except naloxone—the supernatant was subjected to LC-MS/MS. An LCMS-8040 (Shimadzu, Kyoto, Japan) equipped with an LC-20AD HPLC system was used. The mobile phase was 0.1% formic acid and acetonitrile for the detection of acetohexamide, bupropion, doxorubicin, haloperidol, oxcarbazepine, pentoxifylline, and tolperisone metabolites or 10 mM ammonium acetate (pH 5.6) and acetonitrile for the detection of ketoprofen and loxoprofen metabolites. The acetonitrile concentrations used are listed in Table 4. The column temperature was maintained at 40°C. Nitrogen was used as the nebulizer and drying gas. The operating parameters were optimized as follows: nebulizer gas flow, 3 L/min; drying gas flow, 15 L/min; desolvation line temperature, 300°C; and heat-block temperature, 400°C. The other analytical conditions are listed in Table 4. Each metabolite was monitored in the MRM mode. The analytical data were processed using LabSolutions (version 5.82.1; Shimadzu). In loxoprofen and bupropion reductions, *trans*- and *cis*-hydroxyloxoprofen and *threo*- and *erythro*-dihydro bupropion were quantified separately. For tolperisone reduction, two reduced metabolites, *threo*- and *erythro*-dihydrotolperisone, were separately quantified with confirmation of retention time using the metabolites synthesized above. Racemates of licarbazepine, lisofylline, hydroxy acetohexamide, doxorubicinol, reduced haloperidol, and dihydro ketoprofen were observed as single peaks.

To measure naloxone reductase activity, the supernatant was evaluated using an HPLC system (Hitachi, Tokyo, Japan) equipped with an L-2200 autosampler (Hitachi), L-2130 pump (Hitachi), L-2350 column oven (Hitachi), L-2400 UV detector (Hitachi), and D-2500 Chromatographic Integrator (Hitachi). The mobile phase was 20% methanol/50 mM potassium phosphate (pH 6.0), and the column used was Wakopak eco-ODS (4.6 × 150 mm, 5 μm, Wako Pure Chemical). The eluent was monitored at a wavelength of 215 nm. Column temperature was set at 35°C, and the flow rate was 1.0 mL/min. Only 6β-naloxol was detected under the condition in which 6α-naloxol and 6β-naloxol were separated.

Kinetic Analyses. Kinetic analyses were performed using the following ranges of substrate concentrations: acetohexamide, 0–1.5 mM or 0–100 μM; doxorubicin, 0–600 μM; haloperidol, 0–500 μM; ketoprofen, 0–500 μM; oxcarbazepine, 0–50 μM; pentoxifylline, 0–1.0 mM or 0–400 μM; bupropion, 0–200 μM; loxoprofen, 0–500 μM or 0–250 μM; naloxone, 0–250 μM; and tolperisone, 0–400 μM. The kinetic parameters, including K_m, V_{max}, and intrinsic clearance (CL_{int}), were determined using Prism 5 software (Graph-Pad, San Diego, CA).

TABLE 2

Specific peptide sequences used for quantification of each reductase

Protein	Amino Acid Sequence (Position)	Q1/Q3 (m/z)
AKR1C2	SIGVSNFNHR (162–171)	566.0 / 930.5 or 687.3
AKR1C3	DIVLVAYSALGSQR (210–223)	746.6 / 952.5 or 881.5
AKR1C4	DIVLVAHSALGTQR (210–223)	740.6 / 940.5 or 869.5
CBR1	IGVTVLSR (199–206)	423.0 / 731.4 or 575.3
HSD11B1	VIVTGASK (37–44)	387.9 / 562.3 or 463.3

Specific peptide of each protein was detected by MRM mode using two product ions.
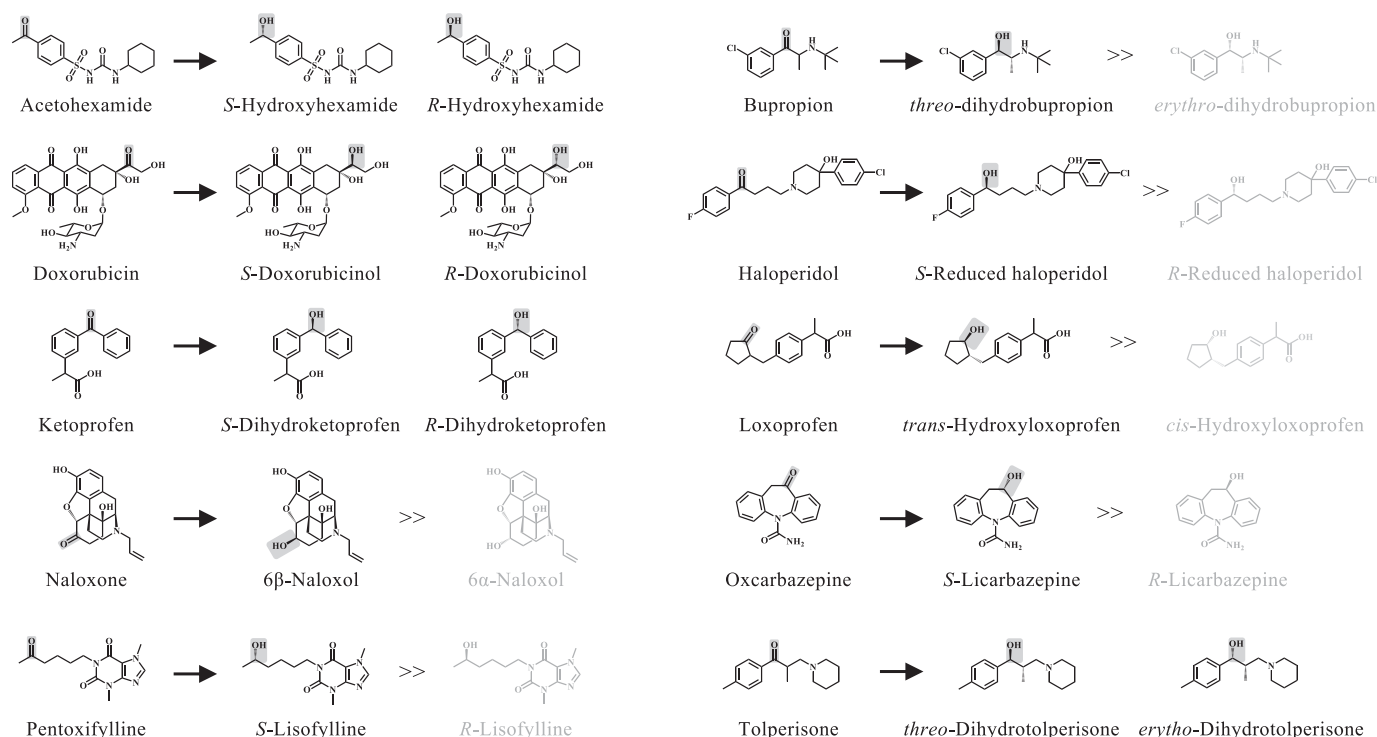
Fig. 1. Chemical structures of 10 test compounds containing a ketone group and reduced metabolites. Ketone groups to be reduced in the substrates, and the corresponding hydroxyl group in metabolites are highlighted in gray color. The color of the chemical structure of minor metabolites is lightened.

Calculation of the Contribution of Each Reductase to Activity in HLC or HLM. The substrate concentrations (15 μM oxcarbazepine, 0.5 μM pentoxifylline, 20 μM acetohexamide, 5 μM loxoprofen, 15 μM doxorubicin, 1.5 μM naloxone, 10 μM haloperidol, 45 μM bupropion, 1 μM ketoprofen, and 10 μM tolperisone) to calculate the contribution of each reductase were determined based on the estimated hepatic maximum concentration of the compound ($C_{inlet,u,max}$) calculated using the following equation:

$$C_{inlet,u,max} = f_u \times \left\{ C_{max} + \left(k_a \times dose \times \frac{f_a}{Q_H} \right) \right\} \qquad (2)$$

where f_u is the unbound fraction in the blood, C_{max} is the maximum concentration in the blood, k_a is the first-order rate constant for gastrointestinal absorption, f_a is the fraction absorbed from the gastrointestinal tract into the portal vein, and Q_H is the hepatic blood flow rate. The pharmacokinetic data used in this study were obtained from previous studies (Chiang and Hawks, 2003; Kang et al., 2011; Elger et al., 2013) or interview forms.

The contribution of each isoform to reductase activity in the human liver cytosol or microsomes was calculated by applying REF. REF was determined as the ratio of the abundance of each reductase in the liver cytosol or microsomes to that of the recombinant enzymes. Using REF and measured reductase activity of the recombinant enzyme ($V_{measured}$), the predicted activity of human liver reductase ($V_{predicted}$) was estimated as follows:

$$V_{predicted} = V_{measured} \times REF \qquad (3)$$

The contribution of each isoform to reductase activity in the liver cytosol ($V_{liver\ cytosol}$) and microsomes ($V_{liver\ microsomes}$) was calculated using the following equation:

$$\text{Contribution} (\%) = \left(V_{predicted} / V_{liver\ cytosol\ or\ microsomes} \right) \times 100 \qquad (4)$$

Statistical Analysis. Statistical significance between two or multiple groups was determined using a two-tailed Student's t test or a two-tailed Tukey's honestly significant difference, respectively. $P < 0.05$ was considered significant.

Results

Reductase Activities for Compounds Containing a Ketone Group by HLC and HLM

Kinetic analyses of the reductase activities of 10 compounds containing a ketone group were performed by HLC and HLM (Figs. 2 and 3). The obtained kinetic parameters are listed in Table 5. In the reduction reactions of six compounds, acetohexamide, doxorubicin, haloperidol, ketoprofen, oxcarbazepine, and pentoxifylline (Fig. 2), reduced metabolites were detected as racemates in single peaks. In reductase activities for five out of six compounds, except for ketoprofen (Fig. 2, A–C, E, and F), HLC showed significantly higher (3.5–13.8-fold) CL_{int} values than HLM, whereas, with respect to ketoprofen reductase activity, HLM showed a significantly higher CL_{int} value (15-fold) than HLC (Fig. 2D). The activities of acetohexamide and pentoxifylline exhibited biphasic kinetics (Fig. 2, A and F), whereas those of doxorubicin, haloperidol, oxcarbazepine, and pentoxifylline exhibited monophasic kinetics (Fig. 2, B–E). In the reduction reactions of the remaining four compounds, bupropion, loxoprofen, naloxone, and tolperisone (Fig. 3), diastereomers of their reduced metabolites were separately detected. In

TABLE 3

Assay conditions for measurement of reductase activity.

Substrate	Substrate Concentration μm	Protein Concentration mg/mL	Incubation Time min
Acetohexamide	100	0.2	30
Bupropion	50	0.05	30
Doxorubicin	150	0.2	60
Haloperidol	50	0.25	60
Ketoprofen	100	0.2	60
Loxoprofen	50	0.2	60
Naloxone	20	0.2	60
Oxcarbazepine	5	0.2	60
Pentoxifylline	100	0.2	15
Tolperisone	100	0.2	60

TABLE 4

Analytical conditions for measurement of reduced metabolites by LC-MS/MS

Reduced Metabolite	Mobile Phase Concentration of Acetonitrile (%)	Column	MRM m/z	CE eV	Flow Rate mL/min
Hydroxyhexamide	5–40 (0–4 min), 40 (4–7 min), 5 (7–9 min)	Develosil[a]	327.15 > 121.05	29	0.2
erythro- or threo-Dihydrobupropion	15	InertSustain[b]	242.05 > 167.95	18	0.2
Doxorubicinol	22	Develosil[a]	546.15 > 399.00	16	0.2
Reduced haloperidol	25	SB[c]	378.15 > 149.00	19	0.2
Dihydroketoprofen	26–70 (0–6 min), 70 (6–12 min), 26 (12–14 min)	Develosil[d]	255.00 > 211.30	8	0.2
trans- or cis-Hydroxyloxoprofen	5–40 (0–8 min), 40 (8–24 min), 5 (24–26 min)	Develosil[d]	246.85 > 203.35	9	0.3
Licarbazepine	0–70 (0–4 min), 70 (4–7 min), 30 (7–9 min)	Develosil[a]	255.10 > 194.00	20	0.2
Lisofylline	30	XDB[e]	281.15 > 263.20	11	0.3
Dihydrotolperisone	40 (0–3 min), 90 (3–11 min), 40 (11–13 min)	XDB[e]	248.20 > 998.10	21	0.2

[a] Develosil ODS-UG-3 2.0 × 150 mm, 3 μm, Nomura Chemical.
[b] InertSustain C18 2.0 × 100 mm, 3 μm, GL Sciences.
[c] SB-C18 2.1 × 50 mm, 3.5μm, Agilent Technologies.
[d] Develosil C30-UG-5 2.0 × 250 mm, 3 μm, Nomura Chemical.
[e] XDB-C8 Eclipse 4.6 × 150 mm, 5 μm, Agilent Technologies.

the reductase activity for bupropion (Fig. 3, A and B), HLC and HLM showed significantly higher (20- and 60-fold, respectively) CL_{int} values of threo-dihydro bupropion formation than those of erythro-dihydro bupropion formation. In threo-dihydro bupropion formation (Fig. 3A), HLM showed a 52-fold higher CL_{int} value than HLC, and their activities exhibited monophasic kinetics. In the reductase activity for loxoprofen (Fig. 3, C and D), HLC and HLM showed significantly higher (7.1- and 8.8-fold, respectively) CL_{int} values with respect to trans-hydroxyloxoprofen formation than those of cis-hydroxyloxoprofen formation. In trans-hydroxyloxoprofen formation (Fig. 3C), HLC showed a significantly (9.1-fold) higher CL_{int} value than HLM, and

their activities exhibited biphasic kinetics (Fig. 3C). With respect to the reductase activity of naloxone (Fig. 3, E and F), only HLC showed 6β-naloxol formation, and the activities exhibited monophasic kinetics. For tolperisone reductase activity (Fig. 3, G and H), the peaks with faster and later retention times in the LC-MS/MS analysis were regarded as diastereomers 1 and 2, respectively. HLC and HLM showed significantly higher (35- and 28-fold, respectively) CL_{int} values for diastereomer 2 formation than for diastereomer 1 formation. For diastereomer 2 formation (Fig. 3H), HLM showed a 24-fold higher CL_{int} value than HLC, and their activities exhibited monophasic kinetics.

TABLE 5

Kinetic parameters for the reduction of each compound by HLC and HLM

Substrate	Reduced Metabolite	Enzyme	K_m μM	V_{max} pmol/min per mg	CL_{int} μL/min per mg
Acetohexamide	Hydroxyhexamide	HLC[1]	100 ± 19	410 ± 40	4.1 ± 0.31
		HLC[2]	3100 ± 340	3400 ± 450	1.1 ± 0.072
		HLM[1]	120 ± 20	53 ± 6.0	0.42 ± 0.040
		HLM[2]	3500 ± 240	440 ± 97	0.12 ± 0.033
Doxorubicin	Doxorubicinol	HLC	130 ± 4.9	280 ± 7.2	2.2 ± 0.29
		HLM	59 ± 3.9	29 ± 8.2	0.48 ± 0.025
Haloperidol	Reduced haloperidol	HLC	85 ± 9.4	380 ± 2.0	4.6 ± 0.49
		HLM	130 ± 13	170 ± 6.2	1.3 ± 0.086
Ketoprofen	Dihydroketoprofen	HLC	NA	NA	0.17 ± 0.0054
		HLM	53 ± 4.4	160 ± 5.3	3.0 ± 0.23
Oxcarbazepine	Licarbazepine	HLC	15 ± 3.6	130 ± 20	8.3 ± 0.81
		HLM	36 ± 5.7	13 ± 1.8	0.36 ± 0.084
Pentoxifylline	Lisofylline	HLC[1]	45 ± 4.9	1300 ± 100	29 ± 1.5
		HLC[2]	160 ± 24	2200 ± 140	14 ± 1.3
		HLM[1]	38 ± 0.49	290 ± 7.3	7.8 ± 0.16
		HLM[2]	200 ± 37	640 ± 14	3.3 ± 0.52
Bupropion	threo-Dihydrobupropion	HLC	44 ± 7.1	28 ± 2.3	0.64 ± 0.14
		HLM	30 ± 17	780 ± 39	31 ± 13
	erythro-Dihydrobupropion	HLC	110 ± 5.3	3.6 ± 0.12	0.035 ± 0.0018
		HLM	34 ± 3.0	18 ± 0.093	0.52 ± 0.011
Loxoprofen	trans-Hydroxyloxoprofen	HLC[1]	250 ± 80	1600 ± 430	6.4 ± 1.6
		HLC[2]	1200 ± 170	5100 ± 580	4.3 ± 0.81
		HLM[1]	120 ± 68	79 ± 15	0.66 ± 0.11
		HLM[2]	1100 ± 160	390 ± 29	0.38 ± 0.022
Loxoprofen	cis-Hydroxyloxoprofen	HLC	180 ± 37	170 ± 19	0.93 ± 0.12
		HLM	810 ± 110	63 ± 10	0.079 ± 0.0031
Naloxone	6β-Naloxol	HLC	37 ± 6.8	470 ± 30	13 ± 2.0
		HLM	ND	ND	ND
Tolperisone	Diastereomer 1	HLC	120 ± 35	1.2 ± 0.24	0.012 ± 0.0017
		HLM	69 ± 4.5	21 ± 0.62	0.30 ± 0.019
	Diastereomer 2	HLC	45 ± 1.3	16 ± 0.21	0.35 ± 0.096
		HLM	61 ± 3.9	510 ± 14	8.5 ± 0.42

NA, not applicable; ND, not detected; HLC[1], high-affinity component; HLC[2], low-affinity component; HLM[1], high-affinity component; HLM[2], low-affinity component.
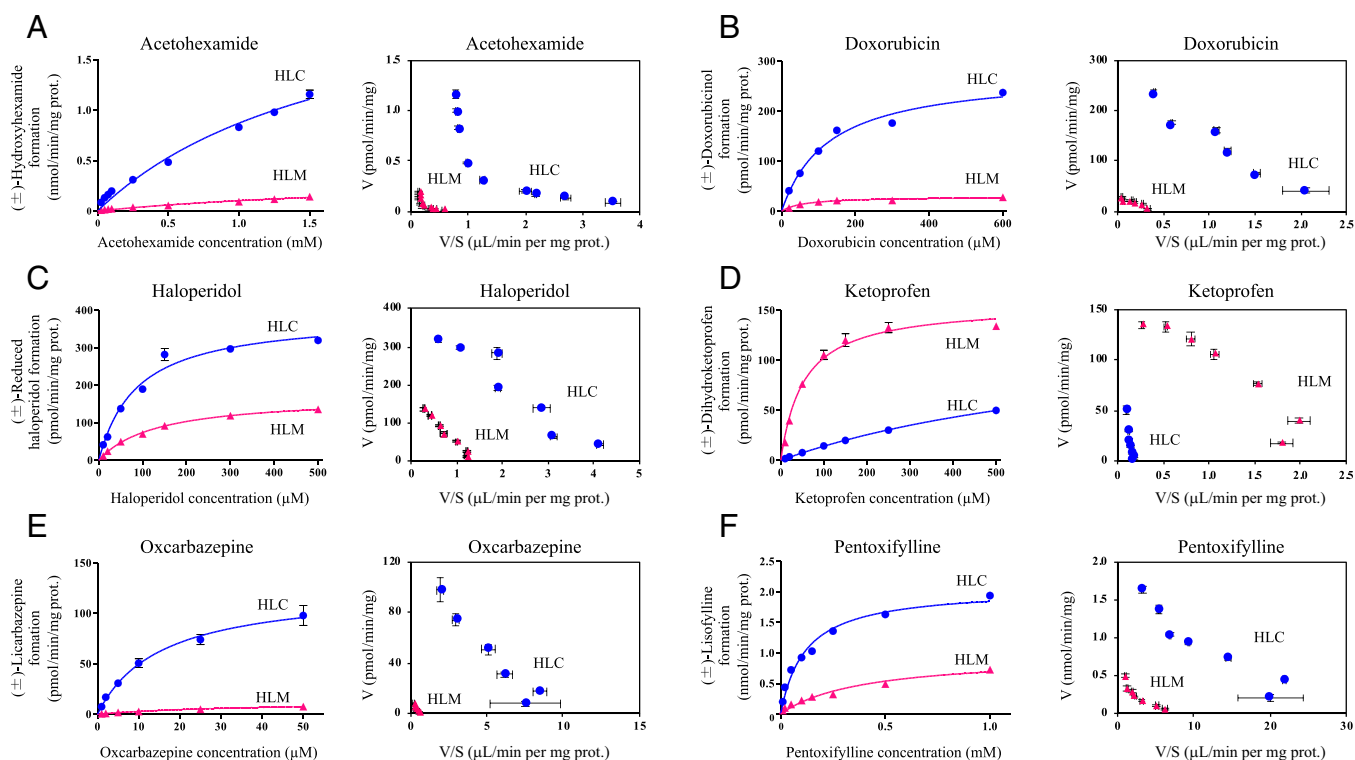
Fig. 2. Kinetic analyses for the reduction of six compounds by HLC and HLM. Substrate concentration vs catalytic velocity (S-V) and Eadie-Hofstee plots of the reductase activities for (A) acetohexamide, (B) doxorubicin, (C) haloperidol, (D) ketoprofen, (E) oxcarbazepine, and (F) pentoxifylline are shown. Each point represents the mean ± S.D. of triplicate determinations. prot., protein; V/S, catalytic velocity/substrate concentration.

Expression of AKR1C1, AKR1C2, AKR1C3, AKR1C4, CBR1, and HSD11B1 Proteins in Expression Systems

To evaluate the catalytic potency of human AKR1C1, AKR1C2, AKR1C3, AKR1C4, CBR1, and HSD11B1, expression systems were constructed for these isoforms. Their expression was examined using immunoblot analysis (Fig. 4). Analysis using anti-AKR1C1 antibody revealed a clear band for rAKR1C1. A clear band for rAKR1C2 and a faint band for rAKR1C4 (Fig. 4A) were also observed, which could be due to the high amino acid identity between AKR1C1 and AKR1C2 (97.8%) or AKR1C4 (82.7%). A band was also observed in the HLC (Fig. 4A). In the analysis using the anti-AKR1C3 antibody, a clear band was observed only in case of rAKR1C3 among the expression systems (Fig. 4B). A clear band was observed in the HLC, and a faint band was observed in the HLM (Fig. 4B). Analysis using an anti-AKR1C4 antibody revealed a clear band in rAKR1C4, but bands were also detected in case of rAKR1C1 and rAKR1C2, and faintly in case of rAKR1C3 (Fig. 4C). The band intensity of the HLC was stronger than that of the HLM. Analysis using an anti-CBR1 antibody revealed three bands for rCBR1 (Fig. 4D). This could be due to modification with 2-oxocarbonyl acid, which does not affect CBR1 activity (Wermuth et al., 1993). Three bands were also observed in the HLC and faintly in the HLM. By analyzing the anti-HSD11B1 antibody, two bands were observed only for rHSD11B1 among the expression systems. A clear band was observed in the HLM. Although a band was also observed in HLC with different mobilities than HLM (Fig. 4E), it would be a nonspecific band because HSD11B1 is a microsomal protein. The mobilities of the bands differed between the HLM and rHSD11B1. HSD11B1 has three potential N-glycosylation sites (asparagine residues at 123, 162, and 207), according to NetNglyc 1.0 (https://services.healthtech.dtu.dk/service.php?NetNGlyc-1.0). Deglycosylation using Endo H caused the band to shift to a higher mobility,

which was matched between HLM and rHSD11B1 (Fig. 4F). Therefore, the difference in mobility between HLM and rHSD11B1 may be due to the difference in N-glycans between HLM and Sf21 cells. Therefore, the expression of each isoform in the constructed expression system was confirmed.

Absolute Expression of Each Reductase Isoform in HLC, HLM, and Expression Systems

To estimate the contribution of AKR1C1, AKR1C2, AKR1C3, AKR1C4, CBR1, and HSD11B1 to the reduction reaction of each compound by HLC or HLM, their expression in the HLC, HLM, and expression systems was quantified by LC-MS/MS targeting the specific peptide of each reductase (Table 6). Unfortunately, AKR1C1 levels were not evaluated because a specific peptide of AKR1C1 could not be determined due to its high amino acid identity with AKR1C isoforms, especially AKR1C2. Among the expression systems of reductases—except AKR1C1—AKR1C3 showed the highest expression efficiency (Table 6). Although AKR1C isoforms are recognized as cytosolic enzymes (Breyer-Pfaff and Nill, 2004), AKR1C2, AKR1C3, and AKR1C4 have also been detected in HLM. CBR1 (recognized as a cytosolic enzyme) and HSD11B1 (recognized as a microsomal enzyme) were specifically detected in HLC and HLM, respectively. In HLC, the expression of AKR1C3 was the highest (159 pmol/mg), followed by that of AKR1C2 (64 pmol/mg), AKR1C4 (51 pmol/mg), and CBR1 (22 pmol/mg). In HLM, the expression of HSD11B1 (73 pmol/mg) was 5.2-fold higher than that of AKR1C3 (14 pmol/mg). The calculated REF values (average) of AKR1C2, AKR1C3, AKR1C4, and CBR1 in HLC were 0.24, 0.14, 0.18, and 0.13, respectively, and those of HSD11B1 in HLM were 0.29. These values were used to calculate the contribution of each reductase to the reduction reactions of the 10 compounds in HLC or HLM.
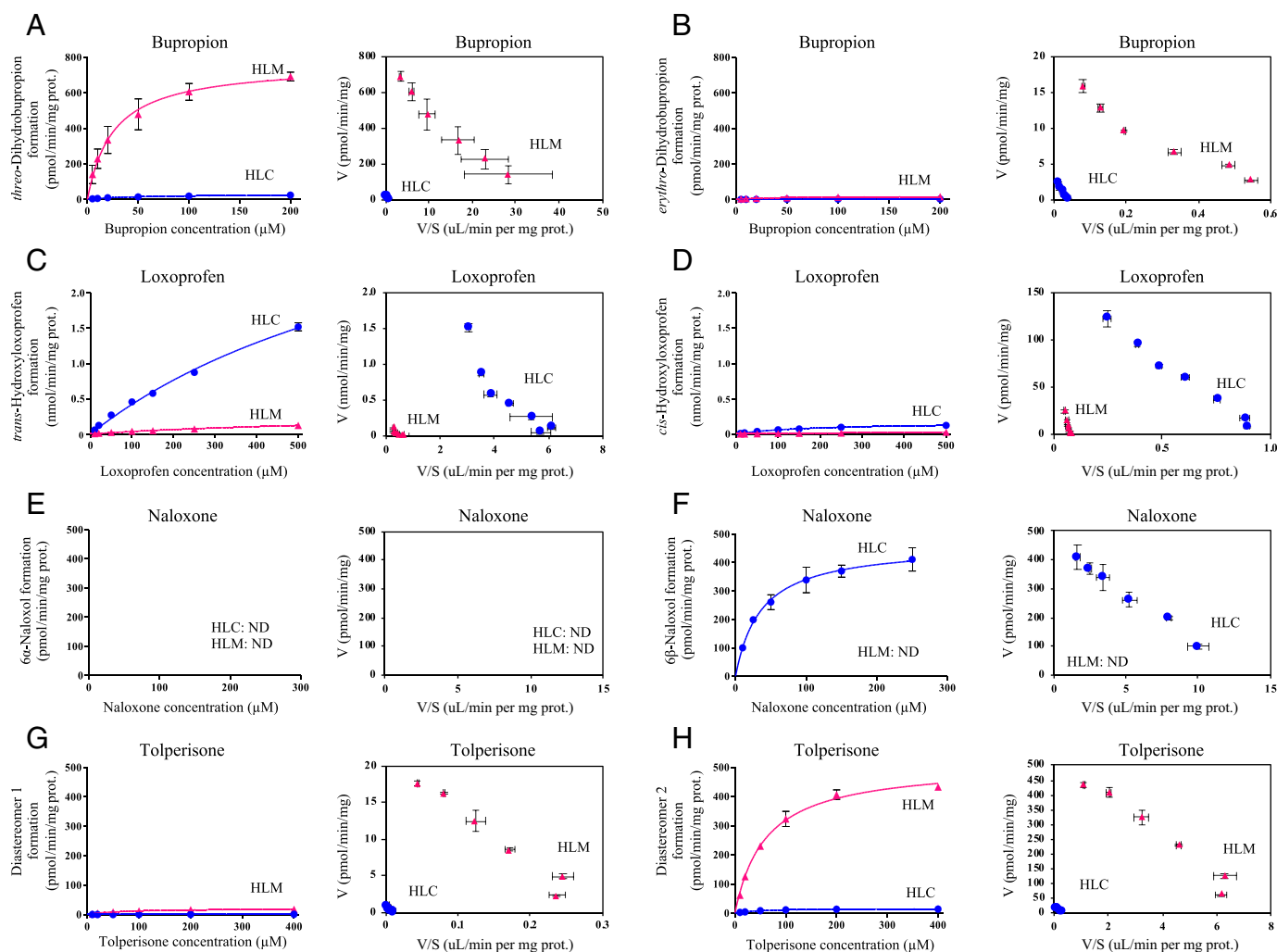
Fig. 3. Kinetic analyses for the reduction of four compounds by HLC and HLM. S-V and Eadie-Hofstee plots of the reductase activities for (A and B) bupropion, (C and D) loxoprofen, (E and F) naloxone, and (G and H) tolperisone are shown. Each point represents the mean ± S.D. of triplicate determinations. ND, not detected; prot., protein; V/S, catalytic velocity/substrate concentration.

Evaluation of Reductase Activities by Recombinant Enzymes and Contribution of Each Reductase to the Reduction Reactions of 10 Compounds in HLC or HLM

To determine the enzyme responsible for the reduction reactions of the 10 compounds in HLC or HLM, the reductase activities of the recombinant reductases were measured at substrate concentrations close to the K_m values in HLC or HLM. Kinetic analyses were performed using recombinant reductases with relatively high activity. To allow comparison with the kinetics of HLC or HLM, the activities of recombinant reductases in the kinetic analyses are shown after normalization using REF (Fig. 5). Finally, the contribution of each reductase to the reduction reactions of the 10 compounds by HLC or HLM was calculated at substrate concentrations corresponding to the estimated hepatic maximum concentrations. In the following sections, the reduction reactions of acetohexamide, doxorubicin, haloperidol, loxoprofen, naloxone, oxcarbazepine, and pentoxifylline, which are mainly catalyzed by enzymes in HLC, were analyzed, and those of bupropion, ketoprofen, and tolperisone, which are mainly catalyzed by enzymes in HLM, were subsequently analyzed.

Acetohexamide Reduction. Acetohexamide reductase activity at 100 μM substrate concentration in HLC was 8.6-fold higher than that in HLM (Fig. 5A). All recombinant reductases showed significantly ($P < 0.001$) higher activities than the mock; in particular, rAKR1C3

and rCBR1 showed relatively high activities (Fig. 5A). The activities of HLC at substrate concentrations from 1 to 100 μM were fitted to the Michaelis-Menten equation, whereas the activities of rAKR1C3 were fitted to the substrate inhibition equation, and those of rCBR1 increased linearly (Fig. 5A). The K_m value of rAKR1C3 (10 ± 0.34 μM) was lower than that of the high affinity component in HLC (100 ± 19 μM) (Table 5 and 7). The contributions of AKR1C3 and CBR1 to acetohexamide reductase activity by HLC at a substrate concentration of 20 μM were 78% and 15%, respectively. These results suggest that AKR1C3 mainly catalyzes the reduction of acetohexamide in the liver. The remaining 7% activity of HLC might be attributed to AKR1C1, AKR1C2, and AKR1C4.

Doxorubicin Reduction. Doxorubicin reductase activity at a substrate concentration of 150 μM by HLC was 9.2-fold higher than that by HLM (Fig. 5B). Among the recombinant enzymes, rAKR1C3 and rCBR1 showed significantly ($P < 0.001$) higher activities than the mock (Fig. 5B). The activities of rAKR1C3 and rCBR1 were fitted to the Michaelis-Menten equation (Fig. 5B). The K_m values of rAKR1C3 (47 ± 3.6 μM) and rCBR1 (200 ± 21 μM) were lower and higher, respectively, than those of HLC (Tables 5 and 7). The contributions of AKR1C3 and CBR1 to doxorubicin reductase activity by HLC at a substrate concentration of 15 μM were 51% and 58%, respectively. These
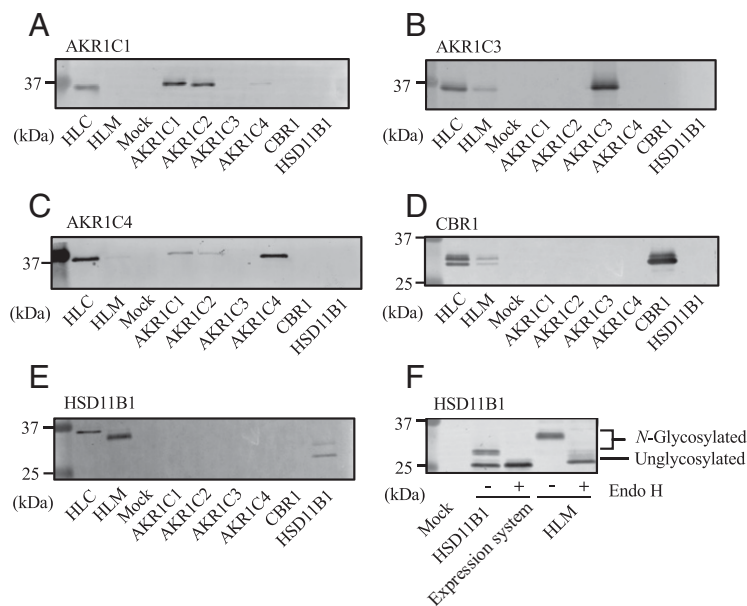
Fig. 4. Immunoblot analyses of AKR1C1, AKR1C2, AKR1C3, AKR1C4, CBR1, and HSD11B1 proteins. HLC, HLM, and recombinant enzymes were separated by SDS-PAGE and probed with (A) anti-AKR1C1, (B) anti-AKR1C3, (C) anti-AKR1C4, (D) anti-CBR1, or (E) anti-HSD11B1 antibodies. (F) rHSD11B1 and HLM treated with Endo H were separated by SDS-PAGE and probed with anti-HSD11B1 antibody.

results suggest that AKR1C3 and CBR1 predominantly contribute to doxorubicin reduction in the liver to the same extent.

Haloperidol Reduction. Haloperidol reductase activity at a 50 μM substrate concentration by HLC was 2.3-fold higher than that by HLM (Fig. 5C). Among the recombinant enzymes, rCBR1 showed prominently high activity, and rHSD11B1 also showed significantly ($P < 0.001$) higher activity than the mock (Fig. 5C). As HSD11B1 is a microsomal reductase, subsequent experiments were performed with a focus on CBR1. The activities of rCBR1 were fitted to the Michaelis-Menten equation (Fig. 5C). The K_m value of rCBR1 (77 ± 6.4 μM) was similar to that of HLC (85 ± 9.4 μM) (Tables 5 and 7). The contribution of CBR1 to haloperidol reductase activity by HLC at a substrate concentration of 10 μM was 97%, suggesting that CBR1 is the only enzyme responsible for haloperidol reduction in the liver.

Loxoprofen Reduction. Loxoprofen reductase activity at a 50 μM substrate concentration by HLC was 25-fold higher than that by HLM (Fig. 5D). Among the recombinant enzymes, rCBR1 showed the highest activity, followed by rAKR1C3 and rAKR1C4 (Fig. 5D). The activity of HLC at substrate concentrations ranging from 1 to 500 μM exhibited biphasic kinetics (Fig. 3C). The activities of CBR1 linearly increased,

the activities of rAKR1C3 fitted to the substrate inhibition equation, and those of rAKR1C4 fitted to the Michaelis-Menten equation (Fig. 5D). The K_m values of rAKR1C3 (140 ± 17 μM) and rAKR1C4 (38 ± 3.5 μM) were lower than those of HLC (250 ± 80 μM) (Table 7). The contributions of AKR1C3, AKR1C4, and CBR1 to loxoprofen reductase activity in HLC at 5 μM were 54%, 34%, and 31%, respectively. AKR1C3, AKR1C4, and CBR1 contributed to loxoprofen reduction in the liver.

Naloxone Reduction. Naloxone reductase activity at a substrate concentration of 20 μM was observed by HLC but not by HLM (Fig. 5E). Among the recombinant enzymes tested, rAKR1C4 showed the highest activity (Fig. 5E). The activities of rAKR1C4 fitted to the Michaelis-Menten equation (Fig. 5E). The K_m value of rAKR1C4 (31 ± 7.4 μM) was similar to that of HLC (37 ± 6.8 μM) (Tables 5 and 7). The contribution of AKR1C4 to naloxone reductase activity by HLC at a substrate concentration of 1.5 μM was 150%. Although there seemed to be some errors in the calculation of the contribution, it was suggested that AKR1C4 is the major enzyme catalyzing naloxone reduction in the liver.

Oxcarbazepine Reduction. Oxcarbazepine reductase activity at a substrate concentration of 5 μM by HLC was 24-fold higher than that

TABLE 6

Expression levels of reductases in pooled HLC, HLM, and expression systems measured by LC-MS/MS

| Protein	MRM m/z	Expression Level (pmol/mg)						REF	REF (Average)
		Expression System	HLC (Average)		HLM (Average)				
AKR1C2	566.0 / 930.5	224	67	(64)	19	(-)		0.30	0.24
	566.0 / 687.3	327	60		ND			0.18	
AKR1C3	746.6 / 952.5	1118	169	(159)	13	(14)		0.15	0.14
	746.6 / 881.5	1229	148		15			0.12	
AKR1C4	740.6 / 940.5	272	54	(51)	15	(-)		0.20	0.18
	740.6 / 869.5	298	49		ND			0.16	
CBR1	423.0 / 731.4	193	22	(22)	ND	(-)		0.11	0.13
	423.0 / 575.4	184	23		ND			0.14	
HSD11B1	387.9 / 562.3	269	ND	(-)	76	(73)		0.28	0.29
	387.9 / 463.3	244	ND		70			0.29	

ND, not detected.
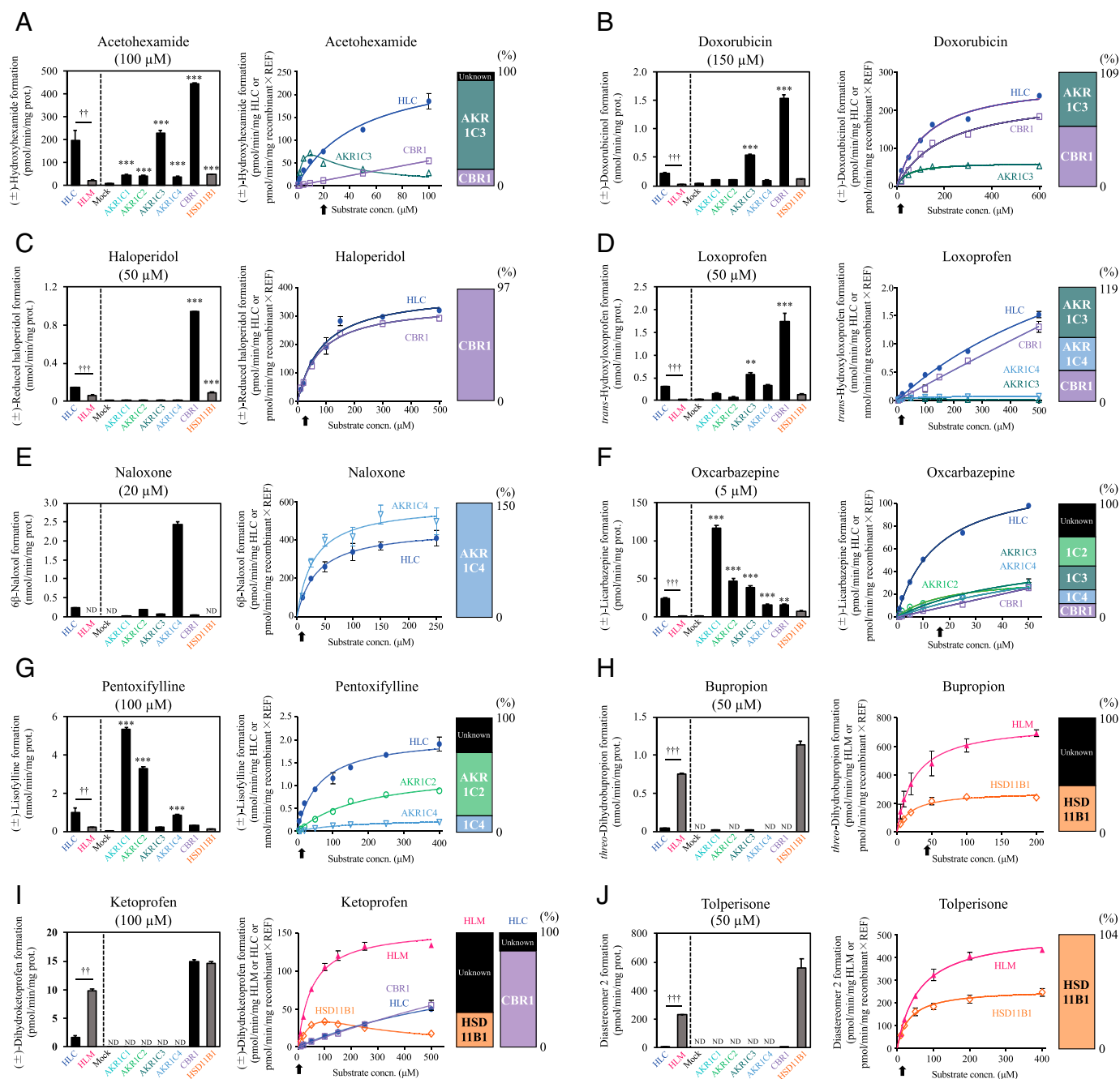
Fig. 5. Reductase activities for 10 compounds by HLC, HLM, and expression systems. Reductase activities by pooled HLC and HLM as well as expression systems were measured at (A) 100 μM acetohexamide, (B) 150 μM doxorubicin, (C) 50 μM haloperidol, (D) 50 μM loxoprofen, (E) 20 μM naloxone, (F) 5 μM oxcarbazepine, (G) 100 μM pentoxifylline, (H) 50 μM bupropion, (I) 100 μM ketoprofen, and (J) 50 μM tolperisone. Kinetic analyses for reduction reactions were performed using (A–G) rAKR1C1, rAKR1C2, rAKR1C3, rAKR1C4, and rCBR1 or (H–J) rHSD11B1. S-V plots by (A–G) HLC and (H–J) HLM are cited from Figs. 2 and 3. The activities of expression systems are shown by normalization using REF values shown in Table 6. The stacked bar chart represents the contribution of each isoform to the activity by HLC or HLM at the substrate concentrations corresponding to the estimated hepatic maximum concentrations (indicated with an arrow in an S-V plot): 15 μM oxcarbazepine, 0.5 μM pentoxifylline, 20 μM acetohexamide, 5 μM loxoprofen, 15 μM doxorubicin, 1.5 μM naloxone, 10 μM haloperidol, 45 μM bupropion, 1 μM ketoprofen, and 10 μM tolperisone. Each column and point represent the mean ± S.D. of triplicate determinations. **$P < 0.01$ and ***$P < 0.001$ compared with the mock (Tukey's honestly significant difference). $^{††}P < 0.01$ and $^{†††}P < 0.001$ (Student's t test). concn, concentration.

by HLM (Fig. 5F). rAKR1C1, rAKR1C2, rAKR1C3, rAKR1C4, and rCBR1 showed significantly ($P < 0.01$) higher activity than those of the mock cells (Fig. 5F). The activities of rAKR1C1, rAKR1C2, and rAKR1C3 fitted the Michaelis-Menten equation, and those of rAKR1C4 and rCBR1 increased linearly (Fig. 5F). The K_m value of rAKR1C1 (5.5 ± 0.41 μM) was lower than that of HLC (15 ± 3.6 μM). The K_m value of rAKR1C2 (20 ± 6.6 μM) was close to that of HLC, and that of rAKR1C3 (56 ± 20 μM) was higher than that of HLC (Tables 5 and 7).

The contributions of AKR1C2, AKR1C3, AKR1C4, and CBR1 to oxcarbazepine reductase activity by HLC at a substrate concentration of 15 μM were 25%, 22%, 12%, and 12%, respectively. The remaining 29% of HLC activity may be attributed to AKR1C1.

Pentoxifylline Reduction. The pentoxifylline reductase activity at 100 μM substrate concentration by HLC was 4.4-fold higher than that by HLM (Fig. 5G). rAKR1C1, rAKR1C2, and rAKR1C4 showed significantly ($P < 0.001$) higher activity than that of the mock control (Fig. 5G).

TABLE 7
Kinetic parameters for the reduction reactions of 10 compounds by recombinant reductases.

Substrate	Enzyme	K_m μM	K_i μM	V_{max} pmol/min per mg × REF	CL_{int} μL/min per mg
Acetohexamide	rAKR1C3	10 ± 0.34	11 ± 0.57	196 ± 3.7	19 ± 0.81
	rCBR1	NA		NA	0.51 ± 0.042
Doxorubicin	rAKR1C3	47 ± 3.6		62 ± 2.3	1.3 ± 0.082
	rCBR1	200 ± 21		240 ± 12	1.2 ± 0.094
Haloperidol	rCBR1	77 ± 6.4		340 ± 1.6	4.5 ± 0.34
Loxoprofen	rAKR1C3	140 ± 17	11 ± 1.3	430 ± 46	3.0 ± 0.094
	rAKR1C4	38 ± 3.5		81 ± 4.7	2.1 ± 0.18
	rCBR1	NA		NA	2.8 ± 0.24
Naloxone	rAKR1C4	30 ± 7.4		590 ± 55	20 ± 3.0
Oxcarbazepine	rAKR1C1	5.5 ± 0.41		ND	ND
	rAKR1C2	20 ± 6.6		37 ± 6.5	2.0 ± 0.40
	rAKR1C3	56 ± 20		65 ± 16	1.2 ± 0.17
	rAKR1C4	NA		NA	0.52 ± 0.032
	rCBR1	NA		NA	0.49 ± 0.024
Pentoxifylline	rAKR1C1	36 ± 3.4		ND	ND
	rAKR1C2	160 ± 9.3		1200 ± 45	7.7 ± 0.19
	rAKR1C4	140 ± 2.1		260 ± 4.0	1.9 ± 0.035
Bupropion	rHSD11B1	20 ± 2.7		280 ± 13	14 ± 1.1
Ketoprofen	rHSD11B1	120 ± 45	97 ± 31	110 ± 33	0.95 ± 0.073
	rCBR1	NA		NA	0.11 ± 0.035
Tolperisone	rHSD11B1	35 ± 8.0		340 ± 19	9.9 ± 1.7

NA, not applicable; ND, not determined, due to no calculation of REF value.

The activities of rAKR1C1, rAKR1C2, and rAKR1C4 fitted to the Michaelis-Menten equation (Fig. 5G). The K_m value of rAKR1C1 (36 ± 3.4 μM) was lower than that of HLC (45 ± 4.9 μM), and that of rAKR1C2 (160 ± 9.3 μM) and rAKR1C4 (140 ± 2.1 μM) was higher than that of HLC (Table 7). The contributions of AKR1C2 and AKR1C4 to pentoxifylline reductase activity by HLC at 0.5 μM were 56% and 14%, respectively. The remaining 30% can be attributed to AKR1C1.

Bupropion Reduction. Bupropion reductase activity at a 50 μM substrate concentration by HLM was 19-fold higher than that by HLC (Fig. 5H). Among the recombinant enzymes, rHSD11B1 showed the highest activity, whereas rAKR1C1, rAKR1C3, and rHSD11B1 showed only marginal activity (Fig. 5H). The activities of rHSD11B1 fitted to the Michaelis-Menten equation (Fig. 5H). The K_m value of rHSD11B1 (20 ± 2.7 μM) was similar to that of HLM (30 ± 17 μM) (Tables 5 and 7). The contribution of HSD11B1 to the bupropion reductase activity by HLM at 45 μM was 41%. It was suggested that microsomal enzyme(s) other than HSD11B1 would also participate in the reduction of bupropion.

Ketoprofen Reduction. Ketoprofen reductase activity at a 100 μM substrate concentration by HLM was sixfold higher than that by HLC (Fig. 5I). Among the recombinant enzymes, rHSD11B1 and rCBR1 showed prominent activity (Fig. 5I). The activity of rHSD11B1 fitted to the substrate inhibition equation (Fig. 3I). The K_m value of rHSD11B1 (120 ± 45 μM) was higher than that of HLM (53 ± 4.4 μM) (Tables 5 and 7). The contribution of HSD11B1 to ketoprofen reductase activity by HLM at 1 μM was 32%, suggesting that microsomal enzyme(s) other than HSD11B1 would also participate in ketoprofen reduction. The activity of rCBR1 linearly increased at substrate concentrations ranging from 1 to 500 μM, which was consistent with that of HLC. The contribution of CBR1 to ketoprofen reductase activity by HLC at a substrate concentration of 1 μM was 84%.

Tolperisone Reduction. Tolperisone reductase activity at a 50 μM substrate concentration by HLM was 27-fold higher than that by HLC (Fig. 5J). rHSD11B1 showed prominent activity, and rCBR1 showed marginal activity (Fig. 5J). The activities of rHSD11B1 were fitted to the Michaelis-Menten equation (Fig. 5J). The K_m value of rHSD11B1 (35 ± 8.0 μM) was lower than that of HLM (61 ± 3.9 μM) (Tables 5 and 7). The contribution of HSD11B1 to tolperisone reductase activity in HLM at 10 μM was 104%, suggesting that HSD11B1 is the only enzyme that catalyzes tolperisone reduction in the liver.

Discussion

The reduction reaction, which is a phase I reaction, is involved in the bioactivation and inactivation of clinical drugs. Although multiple AKR and SDR enzymes often participate in drug reduction reactions, the contribution of each enzyme to the reaction in the human liver has never been quantitatively evaluated. To understand the reasons underlying the contribution of interindividual variability in drug efficacy and susceptibility to drug toxicity, knowledge of the responsibility of each enzyme for metabolism of the concerned drugs would be useful. In this study, the REF approach was used to clarify the contribution of each AKR or SDR isoform to the reduction reactions of 10 compounds that are known to be metabolized via reduction reactions in the human liver.

First, kinetic analyses of 10 compounds were performed (Figs. 2 and 3). In acetohexamide, doxorubicin, haloperidol, loxoprofen, naloxone, oxcarbazepine, and pentoxifylline reduction, HLC showed higher activity than HLM, whereas in bupropion, ketoprofen, and tolperisone reduction, HLM showed higher activity than HLC. The reduction efficiencies of some compounds were compared between HLC and HLM, and the subfractions showing higher activity were consistent with previous reports of haloperidol (Inaba and Kovacs, 1989), pentoxifylline (Lillibridge et al., 1996), oxcarbazepine (Malátková et al., 2014), and bupropion (Connarn et al., 2015). For doxorubicin, Skarka et al. (2011) claimed that microsomal enzymes were also significantly involved in the reduction reaction, because CL_{int} value by HLM (1.0 μL/min per mg) was not much lower than that by HLC (2.1 μL/min per mg). In our study, the CL_{int} value by HLC (2.2 ± 0.29 μL/min per mg) was 4.6-fold higher than that by HLM (0.48 ± 0.025 pmol/min per mg, Table 5). In the liver, the cytosolic protein content is approximately fivefold higher than the microsomal protein content (Tabata et al., 2004); therefore, in either case, cytosolic enzymes would play a significant role in doxorubicin reduction in the liver.

To calculate the contribution of each isoform to the reduction reactions in the liver, the hepatic protein levels of each isoform were quantified by proteomics using LC-MS/MS. Considering the relative protein content between cytosolic and microsomal proteins as described above

(Tabata et al., 2004), the rank order of the protein level of each isoform in the human liver would be as follows: AKR1C3, AKR1C2, AKR1C4, CBR1, and HSD11B1 (AKR1C1 could not be quantified in this study). Our previous study revealed that the rank order of mRNA levels in the human liver is as follows: AKR1C2, AKR1C3, AKR1C1, CBR1, HSD11B1, and AKR1C4 (Amai et al., 2020). As AKR1C4 appears to be highly expressed at the protein level as compared with the mRNA level in the human liver, posttranslational regulation may significantly contribute to its expression.

Acetohexamide reduction was catalyzed by cytosolic enzymes rAKR1C3 and rCBR1, and the contributions of AKR1C3 and CBR1 to the activity in HLC were calculated to be 78% and 15%, respectively (Fig. 5A). Ohara et al. (1995) evaluated the decrease in NADPH at 1 mM acetohexamide and reported that CBR1 purified from the human liver did not catalyze acetohexamide reduction. The inconsistency with our results may be due to the differences in the evaluation methods. As for doxorubicin reduction, it has been reported, by inhibition and correlation analyses using human cytosol samples, that CBR1 rather than AKR1C3 would be a major contributor (Kassner et al., 2008). However, the present study demonstrated that AKR1C3 and CBR1 equally contributed to the reduction in liver function (Fig. 5B). Reduced metabolites of doxorubicin are associated with cardiotoxicity induced by doxorubicin (Olson and Mushlin, 1990; Forrest et al., 2000). As there are 14- and eightfold interindividual variabilities in AKR1C3 and CBR1 at the mRNA level (Amai et al., 2020), individuals with high expression of both isoforms would be at a high risk of developing adverse effects of doxorubicin. Loxoprofen reduction was catalyzed by rAKR1C3, rAKR1C4, and rCBR1, and their contributions to the activity in HLC were calculated to be 54%, 34%, and 31%, respectively (Fig. 5D). Ohara et al. (1995) reported that CBR1 is responsible for the reduction, but they did not analyze whether AKR1C3 has the ability to catalyze it. The present study demonstrated that AKR1C3 largely contributes to the reduction of acetohexamide, doxorubicin, and loxoprofen, which is consistent with the findings of previous studies.

A previous study by Eyles and Pond (1992) demonstrated that only S-(-)–reduced haloperidol is stereoselectively produced from haloperidol in the human liver, although it is not specified whether the metabolite detected in the present study was in the S-form or not. Haloperidol reduction was only observed in rCBR1 (Fig. 5C). This is consistent with a study by Breyer-Pfaff and Nill (2000), who found, using purified enzymes, that the main catalyst for haloperidol reduction is CBR1. As for naloxone reduction, Ohara et al. (1995) reported—by using purified enzymes—that CL_{int} of 6β-naloxol formation from naloxone by AKR1C4 was significantly higher (2.5- or 2.7-fold) than that by AKR1C1 or AKR1C2. The results of the present study demonstrated that naloxone reduction by AKR1C1 and AKR1C2 was scarce, and activity in the human liver was almost entirely explained by AKR1C4 (Fig. 5E). This inconsistency may be explained by differences in evaluation methods, such as measurement of the decrease in NADPH (Ohara et al., 1995) or the production of a metabolite (in this study).

Oxcarbazepine and pentoxifylline reductions were catalyzed by multiple cytosolic isoforms (Fig. 5, F and G), but the sum of their contributions to the activities in HLC did not reach 100%. Jin and Penning (2006) demonstrated that the amino acid residues residing in the substrate binding sites of AKR1C1 and AKR1C2 are almost the same, supported by a high amino acid identity (97.8%, 316 of 323 amino acids). If the contributions of AKR1C1 to the reduction reactions of oxcarbazepine and pentoxifylline are equal to those of AKR1C2 (25% and 56%, respectively), the sum of the contributions of reductases reach 96% and 126%, respectively. Thus, the remaining contribution is likely to be AKR1C1. Although Malátková et al. (2014) reported that rCBR3 can catalyze oxcarbazepine reduction, its contribution to the human liver is negligible because its expression is 230–700-fold lower than that of

AKR1C1, AKR1C2, AKR1C3, AKR1C4, or CBR1 at the mRNA level (Amai et al., 2020). Malátková et al. (2014) reported that in HLC, CL_{int} of the S-licarbazepine formation was 3.7-fold higher than that of R-licarbazepine formation, owing to the lower K_m value, and that AKR1C1, AKR1C2, and CBR1 preferentially produced S-licarbazepine, whereas AKR1C3 and AKR1C4 mainly produced R-licarbazepine. Concordantly, the present study showed that AKR1C1 and AKR1C2 had lower K_m values than AKR1C3, although licarbazepine was detected as a racemate (Table 5). Nicklasson et al. (2002) reported that the area under the curve of S-lisofylline was 38-fold higher than that of R-lisofylline in six healthy volunteers taking 600 mg pentoxifylline, suggesting that the lisofylline detected in the present study might largely be in the S-form.

Bupropion, ketoprofen, and tolperisone were reduced by microsomal reductase HSD11B1 (Fig. 5, H–J). In this study, CL_{int} of $threo$-dihydro bupropion formation in HLM was 60-fold higher than that of $erythro$-dihydro bupropion formation (Table 5), which was consistent with the results of a study by Connarn et al. (2015), who showed that the CL_{int} of $threo$-dihydro bupropion formation was 9.5-fold higher than that of $erythro$-dihydro bupropion formation in HLM. Meyer et al. (2013) also demonstrated that $threo$-dihydro bupropion is preferentially produced in HLM, and recombinant HSD11B1 expressed in HEK293 cells showed the formation. For ketoprofen, it has been reported that recombinant HSD11B1 catalyzes the reduction reaction, although the kinetic parameters have not been calculated (Hult et al., 2001). Here, the role of HSD11B1 in tolperisone reduction in the human liver was clarified (Fig. 5J). HSD11B1 showed different contribution rates to bupropion, ketoprofen, and tolperisone reductions in HLM of 41%, 32%, and 104%, respectively (Fig. 5, H–J). Therefore, microsomal enzymes other than HSD11B1 may also catalyze bupropion and ketoprofen reduction reactions. Another possible reason for the low contribution rates is that the structural difference in N-glycans of HSD11B1 expressed in HLM and Sf21 cells (Fig. 4) affects the specific activity of HSD11B1 for bupropion and ketoprofen reduction. Instead of the REF value, the application of the relative activity factor (Crespi, 1995) may be more reliable for calculating the contribution of each enzyme to the reduction reactions in HLM. To make this feasible, specific substrates must be identified.

To our knowledge, this is the first study to determine the contribution of each reductase to drug reduction in the human liver and to provide a novel finding that AKR1C3 contributes to the reduction reaction of compounds at rates higher than expected.

References

Amai K, Fukami T, Ichida H, Watanabe A, Nakano M, Watanabe K, and Nakajima M (2020) Quantitative analysis of mRNA expression levels of aldo-keto reductase and short-chain dehydrogenase/reductase isoforms in human livers. *Drug Metab Pharmacokinet* 35:539–547.

Bradford MM (1976) A rapid and sensitive method for the quantitation of microgram quantities of protein utilizing the principle of protein-dye binding. *Anal Biochem* 72:248–254.

Breyer-Pfaff U and Nill K (2000) High-affinity stereoselective reduction of the enantiomers of ketotifen and of ketonic nortriptyline metabolites by aldo-keto reductases from human liver. *Biochem Pharmacol* 59:249–260.

Breyer-Pfaff U and Nill K (2004) Carbonyl reduction of naltrexone and dolasetron by oxidoreductases isolated from human liver cytosol. *J Pharm Pharmacol* 56:1601–1606.

Chiang CN and Hawks RL (2003) Pharmacokinetics of the combination tablet of buprenorphine and naloxone. *Drug Alcohol Depend* 70(2, Suppl)S39–S47.

Connarn JN, Zhang X, Babiskin A, and Sun D (2015) Metabolism of bupropion by carbonyl reductases in liver and intestine. *Drug Metab Dispos* 43:1019–1027.

Crespi CL (1995) Xenobiotic-metabolizing human cells as tools for pharmacological and toxicological research. *Adv Drug Res* 26:179–235.

Dalmadi B, Leibinger J, Szeberényi S, Borbás T, Farkas S, Szombathelyi Z, and Tihanyi K (2003) Identification of metabolic pathways involved in the biotransformation of tolperisone by human microsomal enzymes. *Drug Metab Dispos* **31**:631–636.

Elger C, Bialer M, Falcão A, Vaz-da-Silva M, Nunes T, Almeida L, and Soares-da-Silva P (2013) Pharmacokinetics and tolerability of eslicarbazepine acetate and oxcarbazepine at steady state in healthy volunteers. *Epilepsia* **54**:1453–1461.

Eyles DW and Pond SM (1992) Stereospecific reduction of haloperidol in human tissues. *Biochem Pharmacol* **44**:867–871.

Fukami T, Takahashi S, Nakagawa N, Maruichi T, Nakajima M, and Yokoi T (2010) In vitro evaluation of inhibitory effects of antidiabetic and antihyperlipidemic drugs on human carboxylesterase activities. *Drug Metab Dispos* **38**:2173–2178.

Fukami T, Yokoi T, and Nakajima M (2022) Non-P450 Drug-metabolizing enzymes: contribution to drug disposition, toxicity, and development. *Annu Rev Pharmacol Toxicol* **62**:405–425.

Forrest GL, Gonzalez B, Tseng W, Li X, and Mann J (2000) Human carbonyl reductase overexpression in the heart advances the development of doxorubicin-induced cardiotoxicity in transgenic mice. *Cancer Res* **60**:5158–5164.

Honda S, Fukami T, Hirosawa K, Tsujiguchi T, Zhang Y, Nakano M, Uehara S, Uno Y, Yamazaki H, and Nakajima M (2021) Differences in Hydrolase Activities in the Liver and Small Intestine between Marmosets and Humans. *Drug Metab Dispos* **49**:718–728.

Hult M, Nobel CSI, Abrahmsen L, Nicoll-Griffith DA, Jörnvall H, and Oppermann UCT (2001) Novel enzymological profiles of human 11β-hydroxysteroid dehydrogenase type 1. *Chem Biol Interact* **130-132**:805–814.

Inaba T and Kovacs J (1989) Haloperidol reductase in human and guinea pig livers. *Drug Metab Dispos* **17**:330–333.

Jin Y and Penning TM (2006) Molecular docking simulations of steroid substrates into human cytosolic hydroxysteroid dehydrogenases (AKR1C1 and AKR1C2): insights into positional and stereochemical preferences. *Steroids* **71**:380–391.

Kang HA, Cho HY, and Lee YB (2011) Bioequivalence of hana loxoprofen sodium tablet to dongwha loxonin® tablet (loxoprofen sodium 60 mg). *J Pharm Investig* **41**:117–123.

Kassner N, Huse K, Martin HJ, Gödtel-Armbrust U, Metzger A, Meineke I, Brockmöller J, Klein K, Zanger UM, Maser E, et al. (2008) Carbonyl reductase 1 is a predominant doxorubicin reductase in the human liver. *Drug Metab Dispos* **36**:2113–2120.

Kishimoto M, Kawamori R, Kamada T, and Inaba T (1994) Carbonyl reductase activity for acetohexamide in human erythrocytes. *Drug Metab Dispos* **22**:367–370.

Lillibridge JA, Kalhorn TF, and Slattery JT (1996) Metabolism of lisofylline and pentoxifylline in human liver microsomes and cytosol. *Drug Metab Dispos* **24**:1174–1179.

Malátková P, Havlíková L, and Wsól V (2014) The role of carbonyl reducing enzymes in oxcarbazepine in vitro metabolism in man. *Chem Biol Interact* **220**:241–247.

Matsunaga T, Shintani S, and Hara A (2006) Multiplicity of mammalian reductases for xenobiotic carbonyl compounds. *Drug Metab Pharmacokinet* **21**:1–18.

Meyer A, Vuorinen A, Zielinska AE, Strajhar P, Lavery GG, Schuster D, and Odermatt A (2013) Formation of threohydrobupropion from bupropion is dependent on 11β-hydroxysteroid dehydrogenase 1. *Drug Metab Dispos* **41**:1671–1678.

Muta K, Fukami T, Nakajima M, and Yokoi T (2014) N-Glycosylation during translation is essential for human arylacetamide deacetylase enzyme activity. *Biochem Pharmacol* **87**:352–359.

Nicklasson M, Björkman S, Roth B, Jönsson M, and Höglund P (2002) Stereoselective metabolism of pentoxifylline in vitro and in vivo in humans. *Chirality* **14**:643–652.

Ohara H, Miyabe Y, Deyashiki Y, Matsuura K, and Hara A (1995) Reduction of drug ketones by dihydrodiol dehydrogenases, carbonyl reductase and aldehyde reductase of human liver. *Biochem Pharmacol* **50**:221–227.

Olson RD and Mushlin PS (1990) Doxorubicin cardiotoxicity: analysis of prevailing hypotheses. *FASEB J* **4**:3076–3086.

Persson B and Kallberg Y (2013) Classification and nomenclature of the superfamily of shortchain dehydrogenases/reductases (SDRs). *Chem Biol Interact* **202**:111–115.

Skarka A, Skarydová L, Stambergová H, and Wsól V (2011) Anthracyclines and their metabolism in human liver microsomes and the participation of the new microsomal carbonyl reductase. *Chem Biol Interact* **191**:66–74.

Tabata T, Katoh M, Tokudome S, Hosakawa M, Chiba K, Nakajima M, and Yokoi T (2004) Bioactivation of capecitabine in human liver: involvement of the cytosolic enzyme on 5′-deoxy-5-fluorocytidine formation. *Drug Metab Dispos* **32**:762–767.

Wermuth B, Bohren KM, and Ernst E (1993) Autocatalytic modification of human carbonyl reductase by 2-oxocarboxylic acids. *FEBS Lett* **335**:151–154.

Zangar RC, Benson JM, Burnett VL, and Springer DL (2000) Cytochrome P450 2E1 is the primary enzyme responsible for low-dose carbon tetrachloride metabolism in human liver microsomes. *Chem Biol Interact* **125**:233–243.

Address correspondence to: Tatsuki Fukami, Drug Metabolism and Toxicology, Faculty of Pharmaceutical Sciences, Kanazawa University, Kakuma-machi, Kanazawa 920-1192, Japan. E-mail: tatsuki@p.kanazawa-u.ac.jp